The Establishment of Prediction Model for Soil Liquefaction Based on the Seismic Energy Using the Neural Network

yan zhang
Hohai University
wenhui chu (chuwenhui0@foxmail.com)
Hohai University
Mahmood Ahmad
university of engineering and technology peshawar

Research Article

Keywords: Soil liquefaction, Capacity energy, Weak nonlinearity, Prediction model, Neural network

Posted Date: September 15th, 2021

DOI: https://doi.org/10.21203/rs.3.rs-879458/v1

Version of Record: A version of this preprint was published at Environmental Earth Sciences on February 1st, 2022. See the published version at https://doi.org/10.1007/s12665-022-10263-6.

The establishment of prediction model for soil liquefaction based on the seismic energy using the neural network

Yan Zhang[a] , Wen-Hui Chu[b]* , Mahmood Ahmad[c]

[a.]Key Laboratory of Ministry of Education for Geomechanics and Embankment Engineering, and College of Civil and Transportation Engineering, Hohai University, Nanjing 210098, China

[b.]Center for Numerical Simulation Software in Engineering and Sciences, College of Mechanics and Materials, Hohai University, Nanjing 211100, China

[c] Department of Civil Engineering, University of Engineering and Technology Peshawar (Bannu Campus), Bannu 28100, Pakistan

*Corresponding author: chuwenhui0@foxmail.com

Abstract: In the development of the prediction model for soil liquefaction, compared to the stress-based method, the energy-based methods proposed and developed in recent years are closer to the essence of soil liquefaction which is about the energy dissipation. Therefore, considering the weak nonlinear relationship found by the previous research, the fuzzy neural network (FNN) and BP neural network (BPNN) were adopted to try to obtain a prediction model which is the most proper to this nonlinear relationship. Firstly, the database including 284 cases obtained from laboratory test was divided into three separate groups denoted as training, validation set and testing sets by the ratio of 5:1:1; then, the FNN model and BPNN model were iterated to determine the model parameter by referring to the variation of fitness value and relative error of validation set; at the same time, the optimization algorithm of genetic algorithm (GA) was adopted to BPNN to find the best coefficients; besides, the parameter of C_c and D_{50} was respectively excluded from the database to test their influence degree according to the prediction error; finally, 6 prediction results of FNN and genetic algorithm BP neural network (GABP) were compared with the previously proposed models. The results showed that the relationship of capacity energy to the influencing parameters could not be fitted as a fully linear relationship; the FNN model can learn the role of C_c in affecting the capacity energy while the GABP model needs not to take it into account; the FNN and GABP model all fitted

a good weakly nonlinear relationship for the capacity energy, and the GABP model is a better prediction model for capacity energy so far.

Keywords: Soil liquefaction; Capacity energy; Weak nonlinearity; Prediction model; Neural network

Declarations

Funding: There is no funding to support this research.

Conflicts of interest: The authors declare that they have no conflict of interest. Availability of data and material: Not applicable.

Code availability: Not applicable.

All authors contributed to the study conception and design. Material preparation, data collection and the first draft were finished by Yan Zhang; Wen-Hui Chu proposed the idea of this research and calibrated the model parameter; Mahmood Ahmad provided the advice about the AI technology, and revised the first draft. All authors read and approved the final manuscript.

Introduction

Before the engineering design, the geology survey needs to be conducted to evaluate the engineering geological condition, in which the soil liquefaction potential is an important aspect, especially for the high seismic magnitude area. Aiming to this, researchers have proposed many prediction models based on the cyclic stress ratio (CSR) and cyclic resistance ratio (CRR); the typical method is to establish a mathematic formulation to fit the relationship between the CRR, CSR and some macroscopic parameters based on the filed test such as the standard penetration test (SPT) and the cone penetration test (CPT). These stress-based methods are incapable of catching the essence of soil liquefaction, which is the accumulated strain realized by dissipating seismic energy (Azeiteiro et al. 2017; Kokusho 2013, 2017; Tsaparli et al. 2017); the study on the prediction model based on the capacity energy is also conducted simultaneously, however, compared with the stress-based model, it was less focused on. Sonmezer (2019) conducted 36 deformation controlling cyclic simple shear tests to find that the dissipated energy is strongly dependent on relative density and effective stress and concluded a relationship with multiple regression analysis. Dief and Figueroa (2007) studied the influence of relative density and effective confining pressure, as well as the effect of different grain size distribution on the energy per unit volume required for liquefaction; the generalized relationships were obtained by performing regression analyses between the energy per unit volume at the onset of liquefaction and liquefaction affecting parameters. Ni et al. (2020) investigated the variations of the excess pore water pressure ratio and the double-amplitude axial strain with the dissipated energy by conducting a series of undrained cyclic triaxial tests on both loose and medium-dense sand. Jafariavval and Derakhshani (2020) adopted the M50 algorithm to fit the best correlation between parameters and derived formulas with a simple structure. Xiqun Ke et al. (2020) proposed a unified viscous energy dissipation ratio (VEDR) based on the relationship between cyclic stress and strain to study the energy dissipation at each cycle. Millen et al. (2020) presented an energy-based approach for estimating the time to liquefaction; it is directly related to kinetic energy and is uniquely related to liquefaction triggering. At the same time, with the development of artificial intelligence, due to its strong learning capacity, some AI algorithms were adopted to take the

place of the traditional mathematic model, including linear genetic programming (LGP), multi expression programming (MEP), standard genetic programming (GP) (Alavi and Gandomi 2012), adaptive neuro-fuzzy inference system (ANFIS) (Cabalar, Cevik, and Gokceoglu 2012), and the multivariate adaptive regression splines (MARS) (Zhang et al. 2015). Ghorbani and Eslami (2021) used the evolutionary polynomial regression to train an energy-based evaluation model for the liquefaction of sand-clay mixtures using a dataset from shaking table experiments. Pirhadi, Tang, and Yang (2019) applied the response surface method (RSM) to develop six new strain energy models to estimate the capacity energy for soil liquefaction; besides, the effect of fine content was also studied. Pirhadi et al. (2018) obtained a new equation for soil liquefaction evaluation in sandy soil, in which two new earthquake parameters: standardized cumulative absolute velocity and closest distance from the site to the rupture surface (CAV5 and rrup) were introduced. Samui et al. (2015) adopted minimax probability machine regression (MPMR) and extreme learning machine (ELM) for the prediction of seismic liquefaction of soil based on strain energy.

According to the research result above, the relationship between the capacity energy and those measurable parameters is weak nonlinear, be generally fitted as a linear function. However, it will induce an inevitable error if the relationship is purposely fitted as linear. Fortunately, as a supervised learning algorithm, the neural network has a powerful ability of nonlinear interpolation and has been applied to many complicated geotechnical engineering problems. Besides, because the nonlinearity of the fitted model can be controlled by adjusting the structure of the neural network, the technology of the neural network is also tried to evaluate the capacity energy. Baziar and Jafarian (2007) developed an artificial neural network (ANN) model to fit the relationship between soils initial parameters and the strain energy required for liquefaction in sands and silty sands. (Chen et al. 2013) investigated the nonlinear relationship between an increase in pore water pressure and the dissipation of seismic energy through the triaxial shear test of saturated sand and calculate the capacity energy, and presented the principle of nonlinear energy dissipation using an ANN to assess liquefaction potential.

Rahbarzare and Azadi (2019) presented a neuro-fuzzy GMDH (NF-GMDH) model for evaluation of the soil liquefaction

potential through cyclic laboratory tests. Also, the gravitational search algorithm (GSA) was used in this energy-based model.

In this study, two kinds of neural networks, FNN and BPNN, were selected and tried to establish a most reasonable model to predict the capacity energy. To make it convenient to indicate their better prediction performance compared to available models, the dataset containing 284 cases used in the previous research was chosen and divided into three separate groups denoted as training, validation set and testing sets by the ratio of 5:1:1. Besides, the optimization algorithm of GA was adopted to BPNN to find the best initial coefficients. Firstly, the FNN model and GABP model were iterated to determine the model parameter by referring to the variation of fitness value and relative error of every case; simultaneously, the parameter of C_c and D_{50} was respectively excluded to test their influence degree according to their prediction error; then, the performance of FNN and GABP on the testing set were compared and analyzed to indicate the advantage of the later model; finally, 6 prediction results were compared with the previously proposed models to prove the higher accuracy of this newly proposed model.

The introduction of the dataset

the analysis of the determined parameters

According to the established CPT and SPT based model, the essential parameters include the relative density D_r, the effective overburden stress σ' and the fine content FC; for the stratum in certain depth, the σ' can be represented by mean effective stress p' by assuming the lateral stress coefficient is fixed. Except these measurable macroscopic parameters, some mesoscopic parameters characterizing the soil structure also need to be introduced because the energy is dissipated by the friction among soil particles, and it is related to the particle morphology; however, due to the limited measurement technology, the present quantifiable parameters only include the coefficient of uniformity C_u, coefficient of curvature C_c and mean grain size D_{50}. Therefore, these six parameters were determined. In this paper, these parameters'

effect on the dissipated energy were analyzed. The D_r and p' are both related to the contact number and contact force in the soil skeleton, and their increase will compact the soil skeleton to increase the movement resistance of soil grains, increasing the capacity energy under the condition of the same deformation. The variation of FC will influence the soil skeleton structure, with the FC, the sand particle structure is gradually filled with the fine particle, then it transforms to the fine particle structure; at the same time, the CSR firstly increases and then decreases, which means the capacity energy also varied. Besides, the FC also change the C_u, C_c and D_{50}.

The introduction and division of the dataset

In this paper, to collect the capacity energy which can not be obtained in history cases, the data used in this paper was collected by Baziar and Jafarian (2007), including 217 cyclic triaxial (Green, 2001), 61 cyclic torsional shear (Towhata and Ishihara,1995) and 6 cyclic simple shear tests (VELACS project), in which these parameters above can be more accurately measured compared to the field test, improving the performance of the established model. Part of the dataset is presented in Table 1, the capacity energy $Log(W)$ is the output parameter.

Table. 1 The part of the database

p' (kPa)	D_r (%)	FC (%)	C_u	D_{50} (mm)	C_c	W (J)
100.2	81.1	0	1.63	0.46	1.09	10340
100.4	65.3	0	1.63	0.46	1.09	7680
99.11	64.2	0	1.63	0.46	1.09	8260
99.53	64.2	0	1.63	0.46	1.09	7520
100.3	19.6	4	2.45	0.16	0.85	880
99.84	52.1	4	2.45	0.16	0.85	2560
100.8	52.4	4	2.45	0.16	0.85	1740

99.21	52.1	4	2.45	0.16	0.85	2010
100.6	33.7	7	2.46	0.16	0.85	1330
98.05	33.7	7	2.46	0.16	0.85	1770
100.5	27.3	7	2.46	0.16	0.85	2440
101.1	82.1	5	1.64	0.44	1.09	12320
100.8	79.9	5	1.64	0.44	1.09	12160
100.9	81.6	5	1.64	0.44	1.09	11530
101.4	64.7	5	1.64	0.44	1.09	10170
98.48	81	10	1.64	0.42	1.09	22200
99.84	79.7	10	1.64	0.42	1.09	17740
99.95	80.6	10	1.64	0.42	1.09	14350
100.3	62.9	10	1.64	0.42	1.09	11080
99.84	82.1	15	1.65	0.4	1.08	11510
99.53	81.7	15	1.65	0.4	1.08	15340
98.58	62.5	15	1.65	0.4	1.08	6130

The parameter analysis had been conducted by (Alavi and Gandomi 2012; Ghorbani and Eslami 2021), but the parameter C_c was ignored by (Alavi and Gandomi 2012; Jafariavval and Derakhshani 2020; Zhang et al. 2015); besides, the parameter D_{50} was indicated to have a negative effect on the model accuracy in our submitted paper. So, to verify the effect of C_c and D_{50}, other two datasbases excluding these two parameters were trained, respectively.

The databased is randomly divided into three separate groups denoted as training, validation set and testing sets by the ratio of 5:1:1, in which the training set is used to train neural networks; the validation set is used to validate the performance of the training model to avoid the overfitting once the training of nework model has been sucessfully

accomplished; the test set is used to evaluate the generalization ability of the final neural networks and does not participate in the training of the neural networks. In general, the distribution form of the training dataset will affect the calculation efficiency of the gradient descent algorithm, and data preprocessing can improve the solving speed and accuracy. In this paper, the linear normalization method was used.

$$x = \frac{X - X_{min}}{X_{max} - X_{min}} \quad (1)$$

$$y = \frac{Y - Y_{min}}{Y_{max} - Y_{min}} \quad (2)$$

Where X_{max} and X_{min} represent the maximum and minimum value of every input parameter; X is the input value before normalization; x is the normalized input value; Y_{max} and Y_{min} represents the maximum and minimum value of the output parameter; Y is the output value before normalization; y is the normalized output value.

The introduction of the applied neural network

The fuzzy neural network

FNN is established by combining fuzzy theory and neural network; it is equipped with the advantage of neural network and fuzzy technology. Simultaneously, the rule reasoning and fuzzy concept are applied in the node to improve the transparency of the FNN; thus, the ability to interpret, reason and adapt is greatly increased. In this paper, the required structure of FNN is illustrated in Fig. 1.

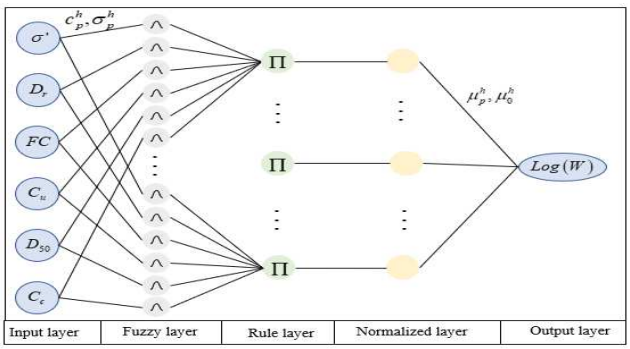

Fig. 1 Fuzzy neural network model for evaluation of capacity energy for soil liquefaction

It can be seen that there are 5 layers in the structure. The first layer is the input layer, and each node represents one parameter;

the second layer is the fuzzy layer which can be calculated as follows:

$$\varphi_p^h = exp\left(-\left(\frac{x_p - c_p^h}{\sigma_p^h}\right)^2\right), (p = 1,\cdots, np; h = 1,\cdots, H_f) \quad (3)$$

Where x_p represents the value of the pth input parameter; φ_p^h is the output of the pth membership function of the hth cluster; c_p^h and σ_p^h is the centre and width of membership function, which is used to evaluate the membership degree of input values to a fuzzy set of the input variables; H_f is the fuzzy partition number, and the total node number of this layer is $\sum_{p=1}^{np} H_f$.

The third layer is fuzzy rule layer matching antecedent of fuzzy rule and calculates applicability of each rule, namely adopting fuzzy operator as a multiplicative operator, its value can be obtained for the second layer following:

$$\Phi^h = \prod_p^{np} \varphi_p^h \quad (4)$$

Where Φ^h is the fitness of the hth fuzzy logic rule of the current layer.

The fourth layer is the normalized layer; its value of each node is the same as that of the third layer, and normalized calculation is realized to avoid oscillation due to excessive modification parameters in the learning process.

$$\overline{\Phi^h} = \frac{\Phi^h}{\sum_{h=1}^{H_f} \Phi^h} \quad (5)$$

Finally, the predicted value is output in the output layer:

$$y_f = \sum_{h=1}^{H_f} \overline{\Phi^h} I^h \quad (6)$$

Where $I^h = \sum_{p=1}^{np} \mu_p^h x_p + \mu_0^h$; y_f is the output value of the normalized capacity energy; μ_p^h and μ_0^h is the parameter of the neuron-fuzzy system.

Multi-layer BP neural network

BP neural network is one of the most widely used and acknowledged artificial neural networks nowadays, typically including an input layer, an output layer, and one or more hidden layers between them, as shown in Fig. 2.

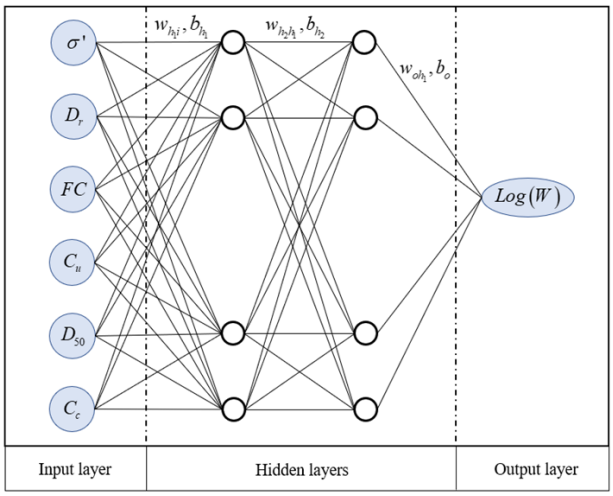

Fig.2 the schematic diagram of BP neural network

156

157 The hyperparameters of the BP neural network, including the number of hidden layers, the number of neurons for each
158 layer, the definition of the objective function, the selection of excitation function, and the approach of initializing weight
159 and bias, all need to be set before network training. During the BP network learning process, the errors are subsequently
160 backwards propagated through the network to adjust the weights and thresholds of the connections between two layers
161 according to the gradient descent algorithm so as to minimize the sum of the absolute error between the output value of the
162 network and the actual output value. BP neural network can theoretically approximate any nonlinear continuous function
163 under the condition of reasonable structure and appropriate weights.

164 The relationship between the input layer and the first hidden layer can be expressed in Eq. (7)

165 $$O_{h_1 i} = f\left(\sum_{i=1}^{np} w_{h_1 i}\, x_i - b_{h_1}\right) \tag{7}$$

166 The relationship between the first hidden layer and the second hidden layer can be expressed in Eq. (8)

167 $$O_{h_2 h_1} = f\left(\sum_{i=1}^{H_1} w_{h_2 h_1}\, O_{h_1 i} - b_{h_2}\right) \tag{8}$$

168 Where $O_{h_1 i}$ and $O_{h_2 h_1}$ represents the output of the first and second hidden layer, when the number of hidden layer is
169 more than two, their relationship is same as Eq. (8). x_i is the normalized input parameter; $w_{h_1 i}$, b_{h_1} and $w_{h_2 h_1}$, b_{h_2}
170 are the weight and threshold of these two hidden layers; np is the input number; H_1 is the number of neuron in the first

hidden layer.

The relationship between the last hidden layer and the output layer is:

$$y_{oh_2} = g\left(\sum_{i=1}^{H_2} w_{oh_2} O_{h_2h_1} - b_o\right) \quad (9)$$

Where y_{oh_2} represents the normalized output value; w_{oh_2} and b_o represent the weight and threshold value of the output layer; H_2 is the number of neuron in the last hidden layer.

The establishment of the prediction model and the performance

As mentioned above, the relationship between the capacity energy and these determined parameters presents weak nonlinearity; according to the fitted linear mathematic formulations collected by (Alavi and Gandomi 2012), their value of the coefficient of correlation R ranges from 0.806 to 0.997. Therefore, while calibrating the model parameter, the neural network structure needs to be carefully tried to avoid the problem of over linearity or over nonlinearity.

The establishment procedure of the FNN model

In this paper, the structure of FNN is a multi-layer of forwarding feedback of local approximation and error backpropagation algorithm, which can be adopted in the network learning and training process. This error is defined as loss function and calculated as follows.

$$e = \frac{\sum_{i=1}^{n}\left(x_i^m - x_i^p\right)^2}{n} \quad (10)$$

where x_i^m and x_i^p represents the actual value and predicted value of the capacity energy; n represents the number of case in the training set and the validation set.

Backpropagation means that if there is a difference between predicted output and actual output, hyperparameters of the last layer will be corrected first, and then the hyperparameter correction procedure will be processed on the input layer. To determine the network coefficient, Levenberg-Marquardt algorithm (LM) was used, which is considered a classic method for optimization. (Asvar, Shirmohammadi, and Barkhordari Bafghi 2018; Leng et al. 2019)

In this paper, the number of the input parameter of three datasets is 6 and 5, respectively; the output index is the capacity energy $\log(W)$, so the $n_p = 6,5$ in the first layer; at the same time, the node number m in the second layer was determined to be 6 by considering the overfitting of the model. The model is trained following steps:

(1) Set the learning ratio $\alpha = 0.001$, correct coefficient $\beta = 0.01$, the maximum iteration number $t = 1000$.

(2) The Gaussian subject function in Eq. (11) was employed because it is able to comprehensive consider the membership of each element and the actual situation.

$$\varphi(x) = gaussian(x, c, \sigma) = \exp(-\left(\frac{x-c}{\sigma}\right)^2) \tag{11}$$

The initial value of c_i^j and σ_i^j is set randomly.

The establishment of the GABP model

Because the performance of the BP neural network depends on the local gradient, and the final training result is determined by the initial weight and bias, the inappropriate initial grid parameter will induce an optimal local solution. In the hybrid optimization algorithm, the GA is a global optimization algorithm to reach the approximate solution of problem search space by simulating biological evolution behavior. As a kind of random search algorithm, GA evolves population through individual hereditary, crossover, and mutation; thereby, it is utilized to optimize the initial value of weight and threshold in BP neural network, as shown in Fig. 3. After obtaining the optimized weight and threshold, they are applied to the BP neural network to be locally optimized to achieve more accurate prediction.

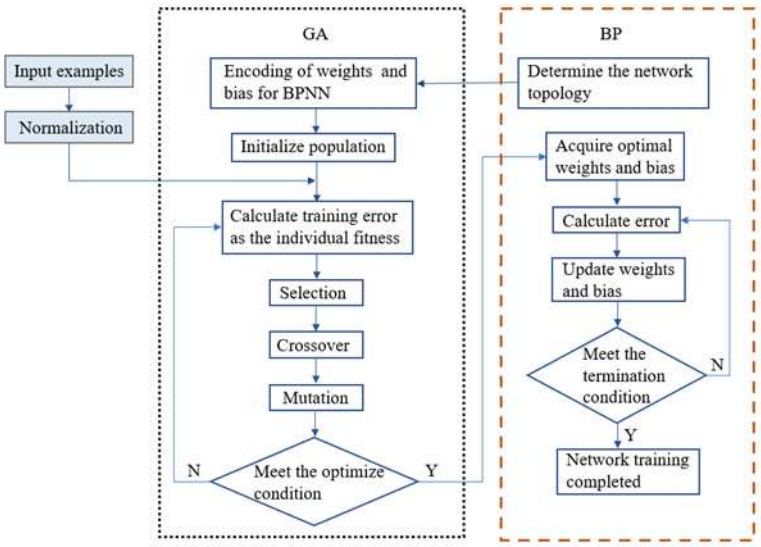

Fig. 3 The flowchart of the GA-BP neural network

209

210 In the GA, the encoding firstly proceeds, and Real-number coding is utilized to avoid the conversion of number systems
211 and long chromosome. In this paper, the chromosome of each individual consists of weights and bias. GA's Fitness function
212 is used to evaluate the superiority and inferiority of each individual.

213

214 $$F = \sum_{i=1}^{n} \left| x_i^m - x_i^p \right| \tag{12}$$

215 where x_i^m and x_i^p represents the actual value and predicted value of the capacity energy; n represents the number of
216 case in the training set and the validation set. Fig. 5(a) illustrates the fitness function value of the best individual in each
217 iteration for GA.

218 In this optimized GA-BP algorithm, Eq. (10) is also applied to evaluate the neural network, and Roulette algorithm is
219 selected for the selection operator. The population size is set as 10 and inherited to the next generation with 10% mutation
220 and 30% crossover fraction; at the same time, 5 generations are employed. In the BP neural network, there is 2 hidden layer
221 with 6 neurons and the learning rate is 0.1. The maximum number of training step is set as 100, and the minimum target
222 error is set as 0.001. The input vector is fully connected to the hidden neurons by a tan-sigmoid transfer function, and the

neurons of the hidden layer are fully connected to the output layer via a linear function.

The accuracy of the established model

In the process of training, three indexes are used to evaluate the model performance, including the coefficient of correlation R, the value of R should be close to one for a good model. (Samui et al. 2015), the root-mean-squared error (RMSE), and mean absolute error (MAE); they are calculated as follows:

$$R^2 = \frac{\sum_{i=1}^{n}(x_i^m)^2 - \sum_{i=1}^{n}(x_i^m - x_i^p)^2}{\sum_{i=1}^{n}(x_i^m)^2} \quad (13)$$

$$RMSE = \sqrt{\frac{\sum_{i=1}^{n}(x_i^m - x_i^p)^2}{n}} \quad (14)$$

$$MAE = \frac{\sum_{i=1}^{n}|x_i^m - x_i^p|}{n} \quad (15)$$

where x_i^m and x_i^p represents the actual value and predicted value of the capacity energy; n represents the number of case in the training set or the testing set.

For the three datasets, the variation of fitness value of two neural networks during the model training is illustrated in Fig. 4 and Fig. 5(b); it can be seen that the number of iterations of BPNN optimized by GA is obviously less than that of FNN, and the initial loss function of BPNN is lower than that of FNN.

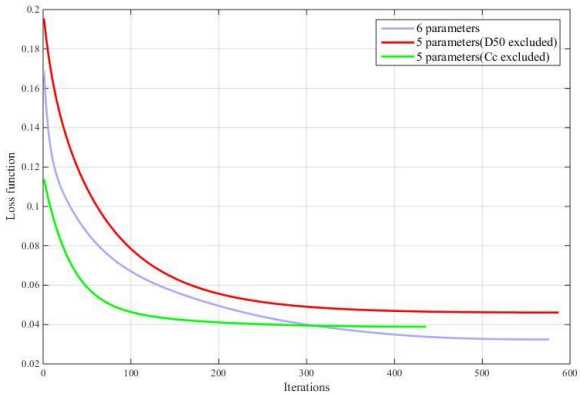

Fig. 4 The variation of loss value of the FNN model during training

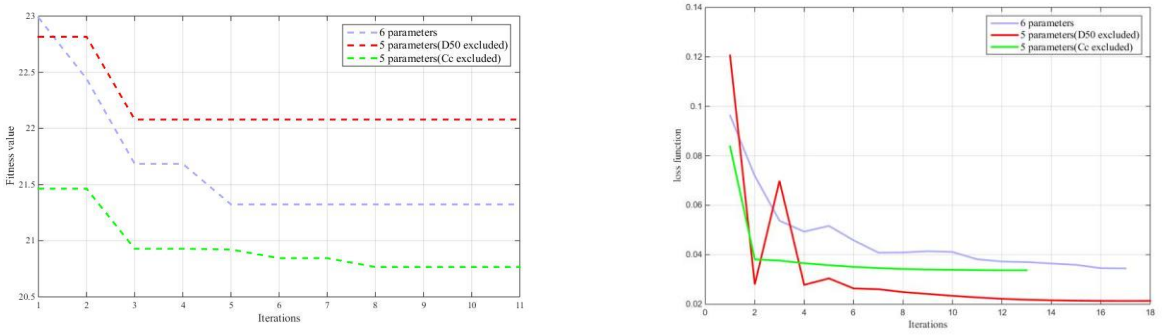

(a) fitness value **(b) loss value**

Fig. 5 The training process of the GABP model

The fluctuation of the prediction error during training is illustrated in Fig. 6-Fig. 8. It can be seen that the process of GABP is more stable than that of FNN even when the other two parameters were excluded; besides, the amplitude of error of GABP was less than FNN. It can also be known that after excluding D_{50} and C_C, the variation of FNN is more intensive than GABP, suggesting that the GABP is more stable during training. As for the GABP model, it can be seen the C_C shows a negative influence on the training progress while the D_{50} contributes to the training and validating process. By contrast, in the FNN model, these two parameters both show the positive effect and the influence of C_C is higher.

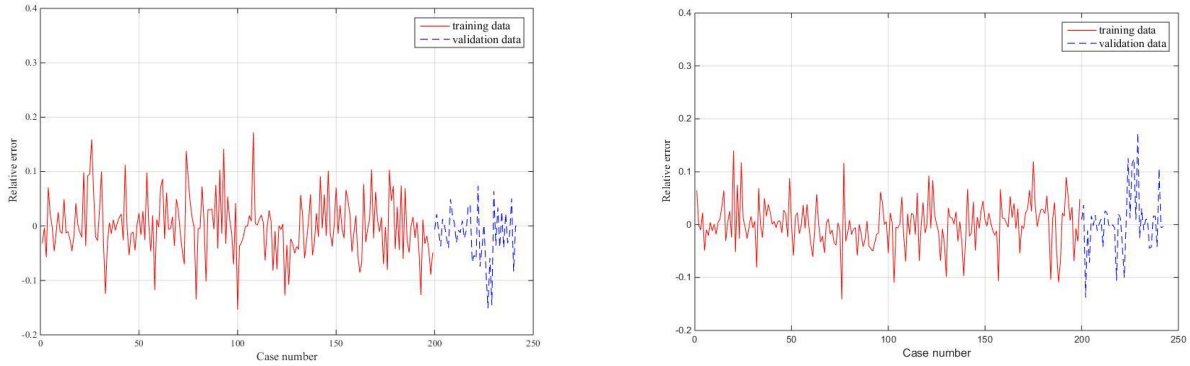

(a) FNN **(b) GABP**

Fig. 6 The fluctuation of prediction error during training

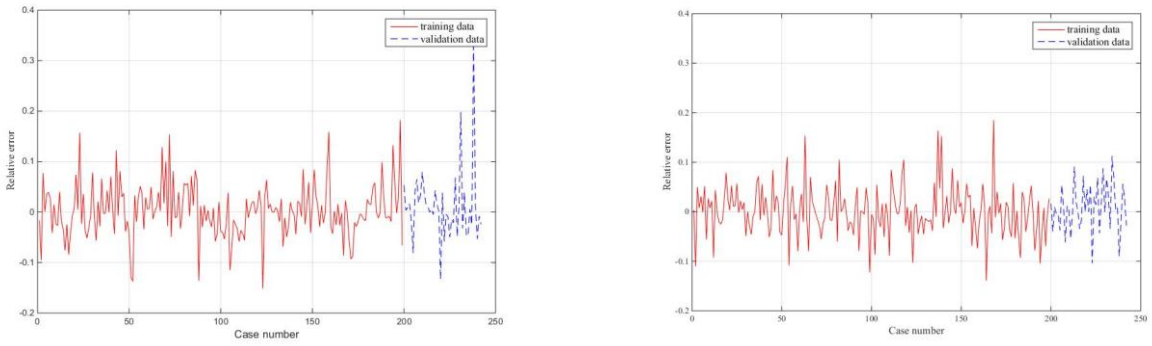

(a) FNN **(b) GABP**

Fig. 7 The fluctuation of prediction error during training (D50 not included)

243

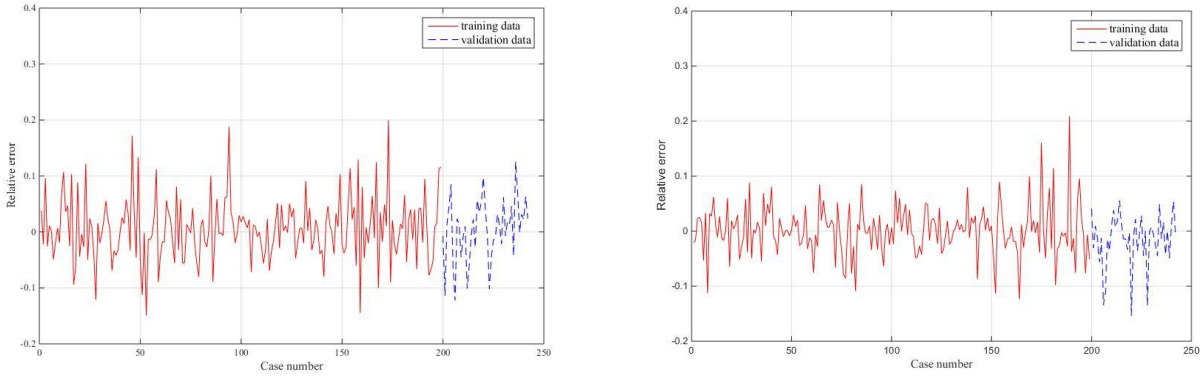

(a) FNN **(b) GABP**

Fig. 8 The fluctuation of prediction error during training (Cc not included)

244 After getting the prediction model, the comparison between the actual and the predicted $\log(W)$ of the test set and the
245 training set is shown in Fig. 9-Fig. 11. It can be seen that the value of R^2 for all models are very close to 1; for the GABP
246 model, the distribution of points more concentrate to the middle line and there is nearly no point locating in the area between
247 10% and 20%, indicating the GABP model performed better than the FNN model. Besides, the red points of the training
248 set and blue points of validation set in GABP model are closer to the middle line, suggesting its learning ability is better
249 than FNN. After excluding the parameter of C_C, for GABP model, the distribution become more concentration while that
250 of the FNN become more disperse, indicating that the presence of C_C disturbed the GABP model learning and the impact
251 of this parameter can not be reflected; by contrast, the FNN can distinct the role of C_C from other two parameters

representing the particle size. After excluding the D_{50}, the point distribution of both FNN and GABP became more disperse, indicating that the relationship of D_{50} with the capacity energy can be leaned by these two models. It is indicated that the GABP can better fit this weak nonlinear relationship. It needs to be noticed that the variation in Fig. 11(a) is more intense than that in Fig. 10(a), indicating in FNN model, the effect of D_{50} is stronger;

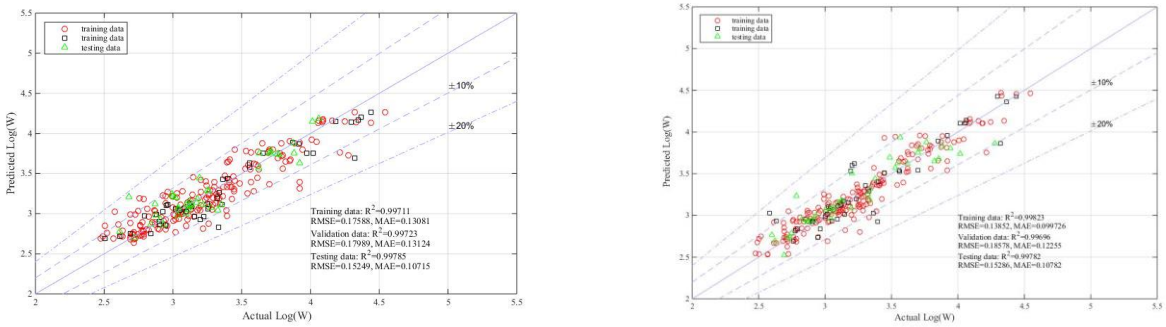

(a) FNN **(b) GABP**

Fig. 9 Comparison between actual and predicted Log(W)

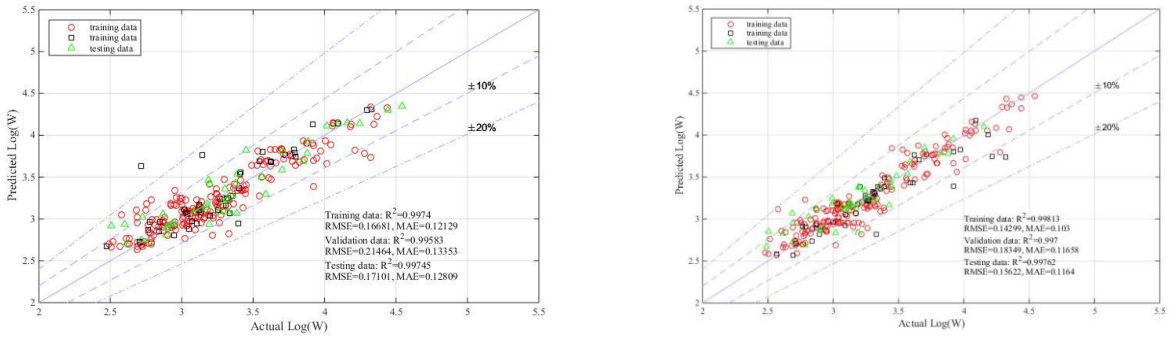

(a) FNN **(b) GABP**

Fig. 10 Comparison between target and predicted Log(W) (D50 excluded)

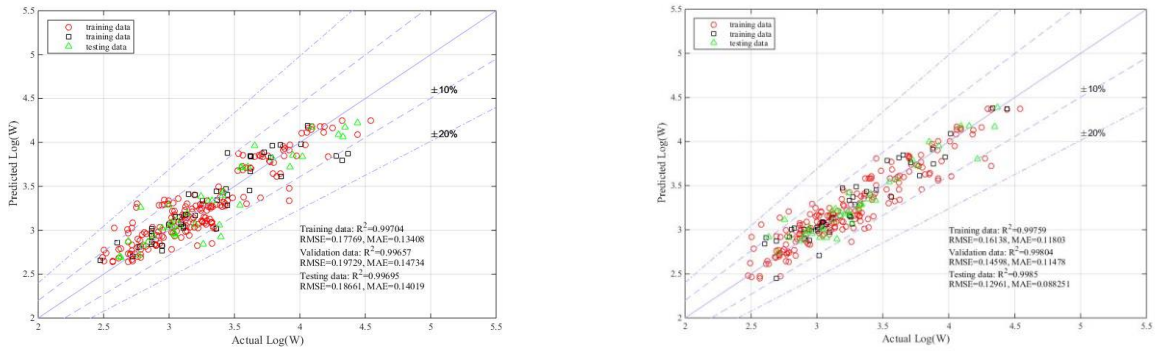

(a) FNN **(b) GABP**

Fig. 11 Comparison between target and predicted Log(W) (C_C excluded)

258

259 The prediction performance of these two models was compared to previous research, as shown in Table. 2. It can be seen
260 the prediction error of the FNN model and the GABP model were mostly lower than others. For models trained by all
261 parameters above, including the MLR, ANFIS, FNN and GABP, the GABP behave best. For models excluding the
262 parameter of C_C, including GP, LGP, MEP, MARS, FNN and GABP, the prediction error of the GABP is still the lowest;
263 besides, some models were trained by huger dataset, it can be indicated that the GABP absolutely is the most appropriate
264 method of machine learning to fit this kind of problem of weak nonlinearity.

Table. 2 The comparison of the model performance

Model	number of cases	RMSE	MAE
MLR(Baziar and Jafarian 2007)	284	0.262	0.213
GP-Cc(Baziar and Jafarian 2007)	399	0.14	0.109
LGP-Cc(Alavi and Gandomi 2012)	301	0.224	0.178
MEP-Cc(Alavi and Gandomi 2012)	301	0.233	0.187
ANFIS(Cabalar et al. 2012)	302	0.181	\
MARS-Cc(Zhang et al. 2015)	302	0.182	0.155

FNN	284	0.152	0.107
FNN-D50	284	0.171	0.128
FNN-Cc	284	0.186	0.140
GABP	284	0.153	0.108
GABP-D50	284	0.156	0.116
GABP-Cc	284	0.130	0.088

Conclusions

In this paper, the prediction model for the capacity energy which can be used to predict the potential of soil liquefaction, was studied. Different from the previous research, the weak nonlinear relationship was noticed and focused on while training the FNN and GABP model. At the time, referring to the author's finding in previous work, their response to the exclusion of parameter of C_C and D_{50} was studied, their prediction performance was also compared to the available models. Finally, the following conclusions can be drawn.

(1) Different from those stress-based prediction models, the relationship of capacity energy to the parameter is weak nonlinear, which cannot be regarded as a similar nonlinear relationship between the CSR and tested in-site parameters.

(2) Comparing with the FNN model, the GABP model does need to consider the effect of C_C.

(3) According to the prediction error, compared to those previously established models, the FNN and GABP model all fitted a good weakly nonlinear relationship for the capacity energy.

(4) For different models, the effect of C_C is different.

Conflicts of interest

The authors declare that they have no conflict of interest.

Acknowledgement

Material preparation, data collection and the first draft t were finished by Yan Zhang; Wen-Hui Chu proposed the idea of this research and calibrated the model parameter. All authors read and approved the final manuscript.

References

Alavi, Amir Hossein and Amir Hossein Gandomi. 2012. "Energy-Based Numerical Models for Assessment of Soil Liquefaction." *Geoscience Frontiers* 3(4):541–55.

Asvar, F., A. Shirmohammadi, and K. Barkhordari Bafghi. 2018. "Predicting Potential of Blast-Induced Soil Liquefaction Using Neural Networks and Neuro-Fuzzy System." *Scientia Iranica* 25(2A):617–31.

Azeiteiro, Ricardo J. N., Paulo A. L. F. Coelho, David M. G. Taborda, and José C. D. Grazina. 2017. "Energy-Based Evaluation of Liquefaction Potential under Non-Uniform Cyclic Loading." *Soil Dynamics and Earthquake Engineering* 92(June 2016):650–65.

Baziar, M. H. and Y. Jafarian. 2007. "Assessment of Liquefaction Triggering Using Strain Energy Concept and ANN Model: Capacity Energy." *Soil Dynamics and Earthquake Engineering* 27(12):1056–72.

Cabalar, Ali Firat, Abdulkadir Cevik, and Candan Gokceoglu. 2012. "Some Applications of Adaptive Neuro-Fuzzy Inference System (ANFIS) in Geotechnical Engineering." *Computers and Geotechnics* 40:14–33.

Chen, Yie Ruey, Jing Wen Chen, Shun Chieh Hsieh, and Yi Teng Chang. 2013. "Evaluation of Soil Liquefaction Potential Based on the Nonlinear Energy Dissipation Principles." *Journal of Earthquake Engineering* 17(1):54–72.

Dief, Hesham M. and J. Ludwig Figueroa. 2007. "Liquefaction Assessment by the Unit Energy Concept through Centrifuge and Torsional Shear Tests." *Canadian Geotechnical Journal* 44(11):1286–97.

Ghorbani, Ali and Amin Eslami. 2021. "Energy-Based Model for Predicting Liquefaction Potential of Sandy Soils Using Evolutionary Polynomial Regression Method." *Computers and Geotechnics* 129(October 2020):103867.

Jafariavval, Yasaman and Ali Derakhshani. 2020. "New Formulae for Capacity Energy-Based Assessment of Liquefaction Triggering." *Marine Georesources and Geotechnology* 38(2):214–22.

Kokusho, T. 2017. "Liquefaction Potential Evaluations by Energy-Based Method and Stress-Based Method for Various Ground Motions: Supplement." *Soil Dynamics and Earthquake Engineering* 95(March 2016):40–47.

Kokusho, Takaji. 2013. “Liquefaction Potential Evaluations: Energy-Based Method versus Stress-Based Method.” *Canadian Geotechnical Journal* 50(10):1088–99.

Leng, Xinke, Huijun Jiang, Xunhao Zou, and Xiaoling Zeng. 2019. “Motion Feature Quantization of Athletic Sports Training Based on Fuzzy Neural Network Theory.” *Cluster Computing* 22:4631–38.

Millen, M. D. L., S. Rios, J. Quintero, and A. Viana da Fonseca. 2020. “Prediction of Time of Liquefaction Using Kinetic and Strain Energy.” *Soil Dynamics and Earthquake Engineering* 128(October):105898.

Ni, Xueqian, Bin Ye, Zirui Cheng, and Guanlin Ye. 2020. “Evaluation of the Effects of Initial Deviatoric Stress and Cyclic Stress Amplitude on Liquefaction Potential of Loose and Medium-Dense Sands: An Energy-Based Method.” *Soil Dynamics and Earthquake Engineering* 136(October 2019):106236.

Pirhadi, Nima, Xiaowei Tang, and Qing Yang. 2019. “Energy Evaluation of Triggering Soil Liquefaction Based on the Response Surface Method.” *Applied Sciences (Switzerland)* 9(4).

Pirhadi, Nima, Xiaowei Tang, Qing Yang, and Fei Kang. 2018. “A New Equation to Evaluate Liquefaction Triggering Using the Response Surface Method and Parametric Sensitivity Analysis.” *Sustainability (Switzerland)* 11(1).

Rahbarzare, Alireza and Mohammad Azadi. 2019. “Improving Prediction of Soil Liquefaction Using Hybrid Optimization Algorithms and a Fuzzy Support Vector Machine.” *Bulletin of Engineering Geology and the Environment* 78(7):4977–87.

Samui, Pijush, Dookie Kim, and R. Hariharan. 2015. “Determination of Seismic Liquefaction Potential of Soil Based on Strain Energy Concept.” *Environmental Earth Sciences* 74(7):5581–85.

Sonmezer, Yetis Bulent. 2019. “Energy-Based Evaluation of Liquefaction Potential of Uniform Sands.” *Geomechanics and Engineering* 17(2):145–56.

Tsaparli, Vasiliki, Stavroula Kontoe, David M. G. Taborda, and David M. Potts. 2017. “An Energy-Based Interpretation of Sand Liquefaction Due to Vertical Ground Motion.” *Computers and Geotechnics* 90(May):1–13.

Xiqun Ke, Junsheng Chen, Weidong Pan, and Yi Shan. 2020. “An Energy-Based Process Evaluation for Low-Plasticity Fine-Grained Soil during Cyclic Loading.” *Geo-Congress 2020 GSP 318* 289–98.

Zhang, Wengang, Anthony T. C. Goh, Yanmei Zhang, Yumin Chen, and Yang Xiao. 2015. “Assessment of Soil Liquefaction Based on Capacity Energy Concept and Multivariate Adaptive Regression Splines.” *Engineering Geology* 188:29–37.